JOURNAL OF PROPULSION AND POWER
Vol. 12, No. 4, July–August 1996

Technical Notes

TECHNICAL NOTES are short manuscripts describing new developments or important results of a preliminary nature. These Notes cannot exceed 6 manuscript pages and 3 figures; a page of text may be substituted for a figure and vice versa. After informal review by the editors, they may be published within a few months of the date of receipt. Style requirements are the same as for regular contributions (see inside back cover).

Stability of Projectiles in Thermally Choked Ram Accelerators

Chiping Li,* K. Kailasanath,† and Elaine S. Oran‡
U.S. Naval Research Laboratory, Washington, D.C. 20375

Introduction

THE ram accelerator[1] is a propulsion concept based on using shock-induced combustion to accelerate projectiles to very high velocities. In a ram accelerator, a projectile travels at supersonic speeds in a launch tube filled with a premixed fuel–oxidizer mixture. Depending on the projectile velocity and the mixture, different forms of shock-induced combustion produce the high pressure on the projectile. If the projectile velocity is greater than the Chapman–Jouget (C–J) velocity of the mixture, oblique detonations can be stabilized on the projectile body[2,3] to generate the high pressure. On the other hand, if the projectile velocity is lower than the C–J velocity, energy released in the combustion in the recirculation region behind the projectile can thermally choke the downstream flow to maintain a high-pressure region on the projectile.[4,5] This high-pressure region provides the needed thrust for projectile acceleration and also controls the projectile stability.

Projectile stability is an importance issue in the ram-accelerator development. An unstable projectile can result in fin erosion, projectile canting, and, ultimately, launch failure. In this study, we focus on projectile stability under the thermally choked condition. Our approach here is to use numerical simulations to analyze the pressure distribution on projectiles that are slightly perturbed from their normal positions to determine if the perturbation is augmented or corrected by the pressure imbalance on the projectile body. The same approach can readily be extended to analyze the stability of projectiles under other conditions.

Physical Models and Numerical Methods

The conservation equations for mass, momentum, energy, and individual species are solved using the flux-corrected transport algorithm (FCT)[6] in conjunction with a two-step, reduced-chemistry model.[7] In the simulations, the virtual cell embedding (VCE)[8] technique is used to accurately represent the complex shape of the ram-accelerator projectile on an orthogonal mesh. The physical models and numerical methods used here have been extensively validated and applied for different flow conditions.[8,9] In this work, two-dimensional, reactive flow simulations were used to provide the pressure information on the projectile. The results obtained from these simulations are not only directly useful to future improvements in the projectile design, but also provide a guide for more comprehensive, three-dimensional studies of this issue.

Results and Discussion

The projectile used in this study is similar to those used in the experiments at the University of Washington,[4] and the geometric specifications of the projectile are shown in Fig. 1. In the simulations, the hydrogen–air mixture (molar fraction, H_2:O_2:N_2/2:1:3.76) was used. The inlet pressure and temperature were 25 atm and 300 K, respectively. The projectile velocity was 1250 m/s and the Mach number was 3.01. In this work, we simulated the flow around projectiles at three different positions. The projectile positions were 1) the center axis of the projectile was at the tube axis, 2) the projectile axis was translated 0.1 cm downward from the tube axis, and 3) the projectile axis was rotated 1.5-deg counterclockwise from the tube axis. The size of the computational domain was 25.0 × 3.8 cm^2. The upper and lower boundaries represented the inner wall of the ram-accelerator launch tube. Two cell sizes, 0.05 and 0.025 cm, were used for the centered projectile and the results show that the solutions were grid-independent. Therefore, the cell size of 0.05 cm was used in all of the simulations.

For each projectile position, we performed three types of simulations.

1) A nonreactive flow simulation: in this case, the pressure profile on the projectile is controlled by the reflected shocks between the projectile surface and the tube wall. These nonreactive simulations provide the baseline results.

2) A reactive flow simulation initiated with a simulated starting process for the thermally choked operation: This numerical starting process produces a pressure pulse similar to that generated in the actual starting process in the experiments using an obturator.[1] A simulation of this type represents a reactive

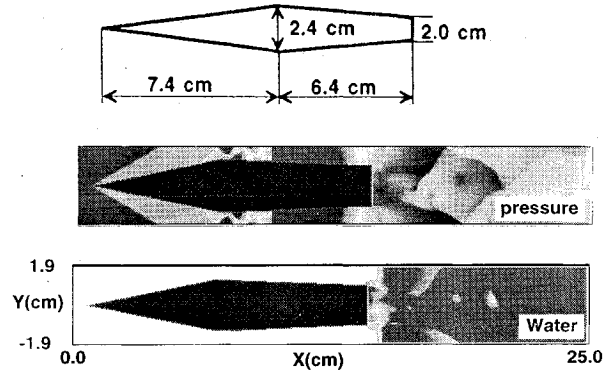

Fig. 1 Schematic of the projectile used in the simulations and the pressure and H_2O vapor concentration fields from the simulation of the reactive flow around the centered projectile.

Received May 20, 1995; revision received Jan. 28, 1996; accepted for publication Feb. 2, 1996.

*Research Scientist, Laboratory for Computational Physics and Fluid Dynamics. Senior Member AIAA.

†Branch Manager, Laboratory for Computational Physics and Fluid Dynamics. Associate Fellow AIAA.

‡Senior Scientist, Laboratory for Computational Physics and Fluid Dynamics. Fellow AIAA.

Table 1 Torque on the projectile from the type-b[a] simulations (N-m per unit length)

	Location of c.m., cm		
Projectile axis	3.4	7.4	11.4
Centered	−4.0 to 3.0	−6.0 to 14.0	−40.0 to 30.0
Translated	2.6 to 5.0 × 10^3	3.0 to 5.4 × 10^2	−2.3 to −1.4 × 10^2
Rotated	−2.2 to −1.5 × 10^4	−9.0 to −5.5 × 10^3	2.8 to 3.2 × 10^3

[a]A normal shock is maintained on the rear of the projectile by thermally choked combustion.

Table 2 Torque on the projectile from the type-c[a] simulations (N-m per unit length)

	Location of c.m., cm		
Projectile axis	3.4	7.4	11.4
Centered	−18.0 to 24.0	−2.0 to 10.0	−3.5 to 2.0
Translated	1.8 to 2.4 × 10^3	3.2 to 4.5 × 10^2	−2.8 to −1.2 × 10^3
Rotated	−5.2 to −3.5 × 10^3	2.3 to −8.5 × 10^3	1.0 to 1.6 × 10^3

[a]No normal shocks are maintained on the rear of the projectile by thermally choked combustion.

flowfield around a ram-accelerator projectile in a successful launch. In this case, the starting pressure pulse generates thermally choked combustion behind the projectile and a normal shock is maintained on the rear part of projectile by the high pressure generated in the combustion process. This shock is crucial for providing the high pressure on the rear part of the projectile for its acceleration.

3) A reactive flow simulation initiated without the simulated starting process: A calculation of this type simulates the flowfield around the projectile in a failed launch in which there are no normal shocks maintained on the rear part of the projectile and, therefore, the projectile decelerates. In this case, there is only a small combustion region behind the projectile base. The energy release from combustion is too weak to choke the flow and the pressure distribution on the projectile is quite similar to that from the nonreactive simulation.

In Fig. 1, we also show the pressure and H_2O vapor concentration (combustion product) around the projectile from the type-b simulation (with the starting process) for the centered projectile to illustrate major flow features. Details of the flowfield can be found in Ref. 10. On the front part of the projectile, there are a series of reflected shock and expansion waves. On the rear part of the projectile, a normal shock is maintained by the high pressure generated in the thermally choked combustion behind the projectile base. The combustion region located behind the projectile is identified by H_2O vapor shown in the figure.

Figure 2 shows the pressure profiles on the projectile from the type-b simulations for the centered, rotated, and translated projectile. These profiles show the location and strength of the normal shock on the projectile. On the centered projectile, the pressure profiles on both the upper and lower surfaces are nearly identical. The peak pressure behind the normal shock reaches as high as 5.5 × 10^4 kPa, which is more than 20 times that of the inlet pressure. On the translated projectile, the locations of the reflected shock and expansion waves are quite similar on both surfaces. The reflected shocks on the front part are stronger and less influenced by the expansion waves on the lower surface than those on the upper surface because of the narrower passage between the lower surface and the wall. Both the strength and location of the normal shocks on the rear part are very close to each other. On the rotated projectile, the pressure profiles on the lower and upper surfaces are very different. The reflected shocks and the normal shock are significantly stronger on the upper surface than their counterparts on the lower surface. Also, the normal shock location is more forward on the upper surface than that on the lower surface, creating a larger high-pressure region.

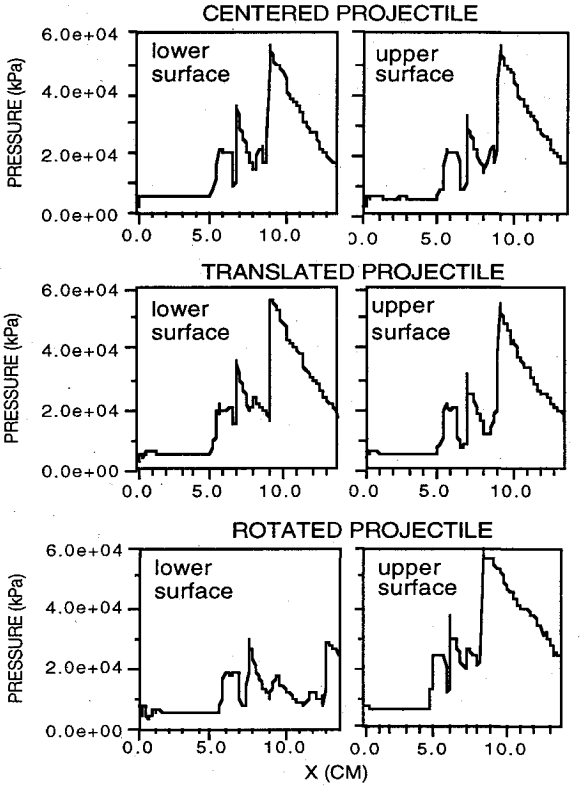

Fig. 2 Pressure distributions on the lower and upper surfaces of the centered, translated, and rotated projectiles from the type-b (with the starting process) simulations.

From the pressure profiles on the projectile, the aerodynamic torque on the projectile was calculated for different c.m. locations of the projectile (3.4, 7.4, and 11.4 cm from the tip). Tables 1 and 2 show the results from the type-b and type-c simulations, respectively. The c.m. location at 7.4 cm from the tip is very similar to that of projectiles used in the experiments.[4] For all three c.m. locations, the aerodynamic torque on the centered projectile is very small from either the type-b or type-c simulation. The torque on the translated projectile is significant for both types of simulations. Therefore, projectile translation leads to projectile rotation (canting). For the forward and middle c.m. locations (3.4 and 7.4 cm from the tip), the aerodynamic torque rotates the projectile counterclockwise and, for the rear c.m. location (11.4 cm from the tip), the

torque rotates the projectile clockwise. On the rotated projectile with the c.m. at 3.4 cm from the tip, the torque is counterclockwise for either the type-b or type-c simulations and, therefore, tends to restore the projectile to its centered position. If the c.m. is at 7.4 cm, the torque is counterclockwise in the type-b simulation and clockwise in the type-c simulation. Therefore, the aerodynamic torque stabilizes the projectile if a normal shock is maintained on the rear part of the projectile and destabilizes the projectile if this shock is absent. On the projectile with the c.m. at 11.4 cm, the torque is clockwise for both types of simulations and, hence, destabilizes the projectile.

Conclusions

We have analyzed the stability of the projectile in the thermally choked ram accelerator based on the pressure information obtained from two-dimensional, reactive flow simulations. The analysis shows that the aerodynamic torque generated by the pressure imbalance because of a perturbation in the projectile position stabilizes the projectile if the c.m. of the projectile is near the projectile tip, and destabilizes the projectile if the c.m. is close to the projectile base. For the projectile with its c.m. located in the middle part of the projectile, similar to the projectile used in the experiments,[4] the aerodynamic torque stabilizes the projectile if a normal shock is maintained on the rear part of the projectile by the thermally choked combustion and destabilizes the projectile if this normal shock is absent. Since this thermally choked shock tends to stabilize the projectile, projectile canting could possibly be more serious in a failed launch process in which no thermally choked normal shocks are maintained on the rear part of the projectile. The normal shock generated by the thermally choked combustion is the key feature of the pressure distribution on the projectile and plays an important role in the projectile stability.

Acknowledgment

This work was supported by the U.S. Air Force Office of Scientific Research and the U.S. Naval Research Laboratory.

References

[1]Hertzberg, A., Bruckner, A. P., and Bogdanoff, D. W., "Ram Accelerator: A New Chemical Method for Accelerating Projectiles to Ultrahigh Velocities," *AIAA Journal*, Vol. 26, No. 2, 1988, pp. 195–203.

[2]Li, C., Kailasanath, K., and Oran, E. S., "Dynamics of Oblique Detonations in Ram Accelerators," *Shock Waves*, Vol. 5, No. 5, 1995, pp. 97–102.

[3]Li, C., Kailasanath, K., and Oran, E. S., "Detonation Structures on Ram-Accelerator Projectiles," AIAA Paper 94-0551, Jan. 1994.

[4]Bruckner, A. P., Knowlen, C., Hertzberg, A., and Bogdanoff, D. W., "Operational Characteristics of the Thermally Choked Ram Accelerator," *Journal of Propulsion and Power*, Vol. 7, No. 1, 1991, pp. 15–26.

[5]Li, C., Kailasanath, K., and Oran, E. S., "Analysis of Transient Flows in Thermally Choked Ram Accelerator," AIAA Paper 93-2187, June 1993.

[6]Boris, J. P., and Book, D. L., "Solution of the Continuity Equations by the Method of Flux-Corrected Transport," *Methods of Computational Physics*, Vol. 16, No. 1, 1976, pp. 85–107.

[7]Oran, E. S., Boris, J. P., Young, T., Flanigan, M., Burk, T., and Picone, M., "Numerical Simulations of Detonations in Hydrogen-Air and Methane-Air Mixtures," *Proceedings of the 18th International Symposium on Combustion*, Vol. 18, The Combustion Inst., Pittsburgh, PA, 1981, pp. 1641–1649.

[8]Landsberg, A. M., Young, T. R., and Boris, J. P., "An Efficient, Parallel Method for Solving Flows in Complex Three-Dimensional Geometries," AIAA Paper 94-0413, Jan. 1994.

[9]Li, C., Kailasanath, K., and Oran, E. S., "Detonation Structures Behind Oblique Shocks," *Physics of Fluids*, Vol. 6, No. 4, 1994, pp. 1600–1605.

[10]Li, C., Kailasanath, K., and Oran, E. S., "Analysis of Stability of Projectiles in Thermally Chocked Ram Accelerators," AIAA Paper 96-0344, Jan. 1996.

Modified Spalart–Allmaras One-Equation Turbulence Model for Rough Wall Boundary Layers

Jaesoo Lee* and Gerald C. Paynter†
Boeing Commercial Airplane Group, Seattle, Washington 98124-2207

Nomenclature

A = constant (=26.0) in van Driest's damping function
k = roughness height
k_s = equivalent sand–grain roughness height
k_s^+ = roughness Reynolds number, $k_s u_\tau/\nu$
u, v = velocity components in the streamwise and the normal to surface direction
u_τ = frictional velocity
x, y = coordinates in the streamwise and the normal to boundary-layer surface directions
θ = momentum thickness
$\varkappa$ = von Kármán constant, 0.41
ν = kinematic molecular viscosity
ν_t = kinematic eddy viscosity

Superscript
$+$ = quantity normalized by ν/u_τ

Introduction

ACOUSTIC lining materials are widely used in inlets and exhaust nozzles to reduce engine noise. These acoustically treated surfaces are aerodynamically rough and cause the turbulent boundary layer to thicken more rapidly than for a smooth surface. Separation locations, the size of the separation bubbles, and the performance of inlets and nozzles all change with roughness. Including surface roughness effects in computational fluid dynamics simulation of fluid flows is, therefore, necessary to improve the accuracy of aerodynamic performance prediction for inlets and nozzles, etc.

The roughness effect on the boundary-layer velocity profile can be accounted for by modifying the eddy dissipation near rough wall surface as suggested by Rotta.[1] Rotta interpreted surface roughness as a reduction of the viscous sublayer. He suggested that the universal law of the wall applies when the plane of reference is shifted in the coordinate direction toward the wall by a small distance R as illustrated in Fig. 1.

Based on the Rotta concept,[1] Cebeci and Chang (C–C) (Ref. 2) developed a roughness model by modifying the inner model of Cebeci and Smith's algebraic turbulence model to include the surface roughness effect. They shifted the reference coordinate system by R toward the wall and calculated the eddy viscosity based on the effective distance from wall, $y + R$:

$$\nu_t = \varkappa^2(y + R)^2 \left[1 - \exp\frac{-(y + R)^+}{A^+}\right]^2 \left|\frac{du}{dy}\right| \qquad (1)$$

where a shift from the wall surface R is a function of k_s^+ and the boundary-layer properties, and was written as

$$R = (0.9\nu/u_\tau)[\sqrt{k_s^+} - k_s^+ \exp(-k_s^+/6)] \qquad (2)$$

Presented as Paper 95-7087 at the 12th ISABE in Melbourne, Australia, Sept. 10–15, 1995; received Oct. 9, 1995; revision received Feb. 12, 1996; accepted for publication Feb. 22, 1996.

*Principal Engineer, Propulsion Research CFD, M/S 49-53. Member AIAA.

†Propulsion Research CFD, M/S 49-53. Associate Fellow AIAA.